

University of Warwick institutional repository: <http://go.warwick.ac.uk/wrap>

This paper is made available online in accordance with publisher policies. Please scroll down to view the document itself. Please refer to the repository record for this item and our policy information available from the repository home page for further information.

To see the final version of this paper please visit the publisher's website.
Access to the published version may require a subscription.

Author(s): John L. West, Anatoliy Glushchenko, Guangxun Liao, Yuriy Reznikov, Denis Andrienko and Michael P. Allen

Article Title: Drag on particles in a nematic suspension by a moving nematic-isotropic interface

Year of publication: 2002

Link to published version:

<http://dx.doi.org/10.1103/PhysRevE.66.012702>

Publisher statement: None

Drag on particles in a nematic suspension by a moving nematic-isotropic interface

John L. West, Anatoliy Glushchenko, and Guangxun Liao
Liquid Crystal Institute, Kent State University, Kent, Ohio 44242

Yuriy Reznikov
Institute of Physics of National Academy of Science, Prospect Nauki 46, Kyiv 252022, Ukraine

Denis Andrienko
Max Planck Institute for Polymer Research, Ackermannweg 10, D-55128 Mainz, Germany

Michael P. Allen
*Department of Physics and Centre for Scientific Computing,
 University of Warwick, CV4 7AL, United Kingdom*
(Dated: May 7, 2002)

We report the first clear demonstration of drag on colloidal particles by a moving nematic-isotropic interface. The balance of forces explains our observation of periodic, strip-like structures that are produced by the movement of these particles.

PACS numbers: 61.30.-v, 61.30.Jf, 64.70.Md, 82.70.-y

Colloidal dispersions of small particles in nematic liquid crystals are a novel, interesting type of soft matter. The difference from ordinary colloids arises from the orientational ordering of the liquid crystal molecules and the resulting structure in the colloid. Topological defects [1, 2, 3, 4] and additional long-range forces between the colloidal particles [5] are immediate consequences of this ordering. The nematic-induced interparticle interaction brings a new range of effects to the system: supermolecular structures [6, 7, 8, 9], cellular structures [10, 11], and even a soft solid [12] can be observed. Colloidal dispersions in liquid crystals also have a wide variety of potential applications [13].

A range of problems similar to those of polymer dispersed liquid crystals also arise in nematic colloidal dispersions. The nematic ordering makes it difficult to suspend small particles in a liquid crystal host. Particles often segregate into agglomerates distributed nonuniformly in the cell. The resulting spatial distribution of the particles is difficult to control. Our research explores the factors that affect the spatial distribution of these particles and indicates ways to control the complex morphology of these systems.

In this paper we report the first demonstration of drag on colloidal particles by a moving nematic-isotropic (NI) interface. We calculate a critical radius above which the particles cannot be captured by the moving interface. We predict that this critical radius is sensitive to the viscous properties of the host liquid crystal, the value of the anchoring coefficient of the liquid crystal on the particle surface, and the velocity of the moving interface. Most important, we can move particles of specified radius and can control the spatial distribution of these particles in the cell.

In order to understand how the particles are moved by the nematic-isotropic transition front we used particles of different size as well as particles made of different

materials. In the first part of our experiments we used nearly monodisperse spheres of silica ($R = 0.005, 0.5$, and $1\mu\text{m}$). To prove our predictions based on initial experimental observations and to demonstrate the controllability of the spatial distribution of particles in anisotropic colloidal suspensions, we used large polymer particles, $R = 8\mu\text{m}$ [17]. In all cases particles were dispersed at concentrations of $\phi = 1 - 5\text{wt } \%$, in the liquid crystal 5CB at room temperature (25°C) (the isotropic-nematic transition temperature of pure 5CB is $T_{\text{NI}} \approx 35^\circ\text{C}$). The sample was subjected to ultrasound in order to uniformly disperse the particles in 5CB. Some of the preparations were made at higher temperatures, in the nematic or isotropic state of the liquid crystal.

The homogeneous mixture was deposited between two polymer-covered glass substrates and heated above the nematic-isotropic transition point. The cell thickness was $100\mu\text{m}$. The homogeneous suspension was observed under crossed polarizers using an optical microscope, Fig. 1a.

The mixture was cooled to a temperature below the transition point. Depending on the rate of cooling, we observed different structures. Fast quenching to room temperature (cooling rate $10^\circ\text{C min}^{-1}$) resulted in phase separation and formation of a cellular structure, with particle-free nematic domains separated by particle-rich regions, Fig. 1b. Properties of these structures have been reported previously [10, 11, 12]. Decreasing the cooling rate, we observed formation of a striped structure (Fig. 1c). The particle-rich regions were no longer forming a cellular structure but were arranged in a set of stripes, separated by particle-free regions. Using optical microscope images we postulate that we have large nematic and isotropic domains separated by a moving interface. The direction of the stripes is parallel to the moving interface (the interface was moving from the left to the right of the cell in the geometry depicted in Fig. 1).

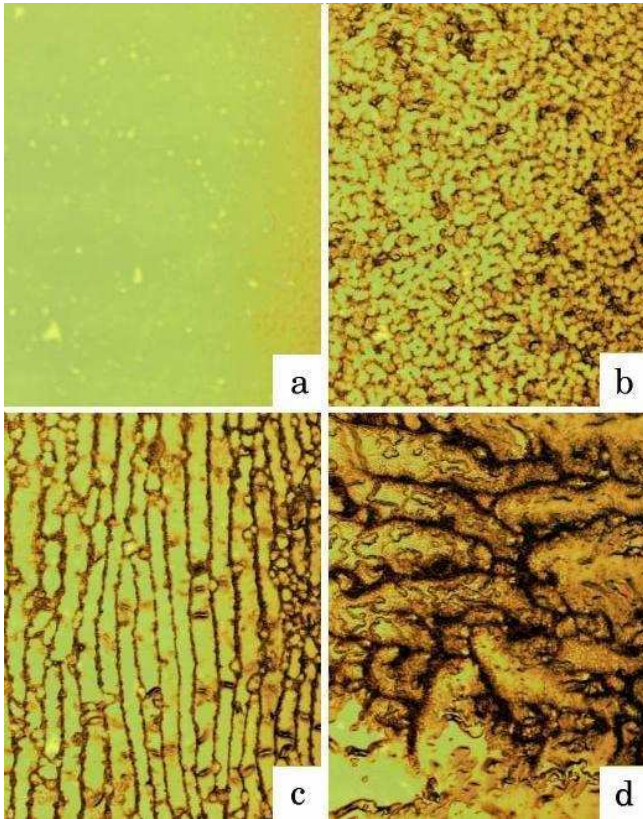


FIG. 1: Polarized microscopy images of different structures, depending on the cooling rate: (a) colloidal particles are dispersed homogeneously in the isotropic phase; (b) *cellular* structure: cooling rate 10^0C min^{-1} ; (c) *stripes*: cooling rate 0.1^0C min^{-1} , velocity of the interface $v \approx 3 \mu\text{m sec}^{-1}$; (d) *root* structure: cooling rate 0.01^0C min^{-1} , $v \approx 0.5 \mu\text{m sec}^{-1}$. Silica particles, $R = 0.005 \mu\text{m}$, concentration $\phi = 1 \text{wt \%}$. The NI interface is moving from the left to the right. The long side of the images is 1mm.

The spatial period of the striped structure depended on the cooling rate, as well as on the particle size. Increasing the particle size, as well as decreasing the cooling rate, resulted in an increase of the spatial period. We also noticed that the stripes do not appear if we have considerably larger silica particles, $R > 0.5 \mu\text{m}$. Also, decreasing the cooling rate resulted in a chaotic merging of stripes and formation of a “*root*”-like pattern, Fig. 1d. These results indicate that the particles are pushed by the moving nematic-isotropic phase transition front.

Using optical microscopy we were able to directly observe the movement of larger ($R = 8 \mu\text{m}$) but less dense polymer spheres. We could see these particles being moved by an advancing nematic to isotropic phase boundary. Fig. 2 shows pictures of this moving front taken at different times. Clearly the particles are pushed by this advancing front, remaining in the isotropic phase.

A simple analysis accounts for these experimental observations. We consider several mechanisms which contribute to the total drag force acting on a particle at

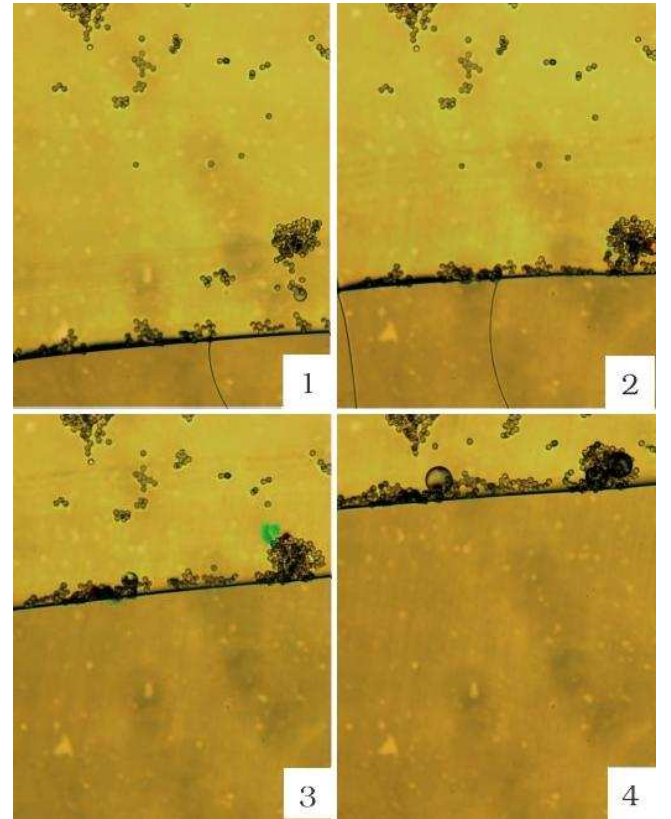


FIG. 2: Snapshots of the moving nematic-isotropic interface made between parallel polarizers taken with the time interval $\Delta t = 6 \text{min}$. The nematic phase is on the bottom part of the picture. Polymer particles, $R = 8 \mu\text{m}$. One can observe thickening of the particle-rich phase because of the capturing of the particles by the interface. Velocity of the interface is $v \approx 3 \mu\text{m sec}^{-1}$. The long side of the images is 1mm.

a NI interface. First, the surface tension coefficient might differ at the particle-nematic or particle-isotropic part of the interface. An additional pressure caused by the curvature can be given by $P = 2\sigma/R$, where R is the radius of the curvature (in our case it is the radius of the particle) and σ is the surface tension coefficient. This pressure contributes to the total drag force as $F_\sigma = 2\pi(\sigma_N - \sigma_I)R[1 - (d/R)^2]$, with the amplitude growing linearly with the droplet radius. Here d is the distance from the particle center to the interface. The value of $\Delta\sigma = \sigma_N - \sigma_I$ depends on the surface treatment of the particles and is unknown (and difficult to measure) for our system. However, the order of magnitude can be estimated from the change of the surface tension coefficient of the glass-5CB interface [14], $\Delta\sigma \approx 10^{-2} - 10^{-3} \text{dyne cm}^{-2}$.

Second, the particle creates long-range distortions of the director in a nematic phase. To minimize elastic distortion energy, the nematic tries to expel particles into the isotropic phase. The elastic forces have two origins: due to the director deformations in the bulk nematic and due to the anchoring of the director at the particle sur-

face. An estimation of these contributions can be done by dimensional analysis. For the surface contribution, the only combination which has dimension of force is WR , where W is the anchoring coefficient. Therefore, the surface contribution to the drag force is proportional to WR , $F_s = WRg_s(d/R)$, where $g_s(x)$ is a dimensionless function of the penetration depth, d/R .

One can have two different situations for the bulk contribution. For *weak* anchoring, $WR/K \ll 1$, the bulk contribution is proportional to the squared characteristic deviation of the director, $\beta_0 \sim WR/K$ [15]. Now $W^2 R^2 / K$ has the dimension of force, yielding $F_b = W^2 R^2 / K g_b(d/R)$. In contrast, in the case of strong anchoring, $WR/K \gg 1$, the anchoring does not enter the elastic contribution, and $F_b = K g_b(d/R)$. Here, again, $g_b(x)$ is a dimensionless function. For 5CB [18], and typical values of the anchoring energy, $W \approx 10^{-3} - 10^{-4}$ dyn cm⁻¹, $WR/K \ll 1$ for silica particles and $WR/K \approx 1$ for polymer particles. Therefore, for silica particles, we have the weak anchoring regime. In contrast, polymer particles provide strong anchoring of the director. We also note that, when particles agglomerate, the effective radius increases and we have a strong anchoring regime even for small particles.

Finally, there is a friction drag contribution, which, in the first approximation, is given by the Stokes formula, $F_\eta = -6\pi R\eta v$ [16]. The total drag on the particle is the sum of all contributions, $F_{\text{drag}} = F_\sigma + F_b + F_s + F_\eta$.

Solution of Newton's equations of motion with F_{drag} as a force completes the description of the particle dynamics. It is clear, however, that small heavy particles cannot be moved by the interface. The maximal radius can be estimated from the conservation of linear momentum. To capture a particle of mass m , the interface has to transfer to it a linear momentum mv . If we assume that the particle does not move (or it moves much slower than the interface, which is valid for massive particles) then the total linear momentum transferred to the particle reads

$$mv = \int_{t_1}^{t_2} F_{\text{drag}} dt = \frac{1}{v} \int_{-R}^R F_{\text{drag}}(x) dx, \quad (1)$$

Here we assumed that the interface touches the particle at time t_1 and leaves it at time t_2 , $x = vt$. Substituting F_{drag} we obtain

$$R_{\max} = \frac{\frac{8}{3}\pi\Delta\sigma + \delta_s W - 6\pi\eta\Delta r}{\frac{4}{3}\pi\rho v^2 - \delta_b W^2 / K}, \quad (2)$$

where δ_i are geometrical constants, ρ is the density of the particle, Δr is the final displacement of the particle due to the drag force.

Several important conclusions can be drawn. First, if the particle is too big, the moving interface is not able to transfer sufficient linear momentum to it. Only particles with $R < R_{\max}(v, W, \sigma)$ will be captured by the interface. From eqn (2) one can see that $R_{\max} \propto v^{-2}$, i.e. only a slowly moving interface is able to capture the particles. The estimate of this velocity is given by the zero of

the denominator of eqn (2), $v \approx W/\sqrt{K\rho} \sim 1$ mm sec⁻¹. This is of the order of the limiting velocity for the cellular structure we observed in our experiments: if the interface moves more slowly, then stripes appear, otherwise the cellular structure forms (see Fig. 1).

The main conclusion is that R_{\max} is a function of the material parameters, i.e. can be effectively controlled, for example, by changing the surface treatment of the particles (anchoring energy W). Increase in the anchoring energy leads to an increase of R_{\max} . Moreover, strong enough anchoring favors formation of a defect near the particle [1, 6], contributing to an even higher energetic barrier created by elastic forces.

On the other hand, if the particle is captured by the interface, the elastic force scales as R^2 , and the opposing viscous drag scales as R . Therefore, there is a minimal radius, R_{\min} , starting from which particles will be dragged by the interface. If the particle is dragged by the interface at a constant speed, then $F_{\text{drag}} = 0$, yielding

$$R_{\min} = \frac{6\pi\eta v - 2\pi\Delta\sigma - \gamma_s W}{\gamma_b W^2 / K}, \quad (3)$$

where $\gamma_i = g_i(0)$ are some constants. Eqn (3) implies that, in order to be moved by the interface, the particles have to be big enough. Only in this case can elastic forces overcome viscous drag. Substituting values typical for 5CB and using the slowest cooling rate, we obtain $R_{\min} \approx 0.01\mu\text{m}$ which qualitatively agrees with the minimum size of silica particles we were able to move.

To explain formation of the striped structure, we note that, in practice, particles aggregate into clusters. While an aggregate moves, it captures more and more particles, growing in size. The anchoring parameter WR/K also increases and we switch from the weak anchoring to the strong anchoring regime. The bulk elastic contribution is then proportional to the elastic constant K and the elastic force is no longer growing as R^2 . Therefore, at some R_c , the friction drag overcomes the elastic contribution and the aggregate breaks through the interface. A stripe forms and the particles start to accumulate again. The condition $F_{\text{drag}} = 0$ gives the critical size of the aggregate

$$R_c = \frac{\gamma_b K}{6\pi\eta v - 2\pi\Delta\sigma}, \quad (4)$$

which is about $1\mu\text{m}$ for typical experimental values.

From conservation of mass one can show that the radius of the aggregate increases linearly with time until it reaches R_c ,

$$R = R_0 + \frac{1}{4}\phi \frac{\rho_{LC}}{\rho_a} vt. \quad (5)$$

Here R_0 is the initial radius of the aggregate, ρ_a is the density of the aggregate. Therefore, the distance between two stripes is given by

$$\lambda \approx 4\phi^{-1} \frac{\rho_a}{\rho_{LC}} R_c, \quad (6)$$

and is of the order of 0.1mm, again in qualitative agreement with experiment, Fig. 1.

In conclusion, we have demonstrated moving colloidal particles by a moving nematic-isotropic interface. We have also determined the factors such as particle size, anchoring energy and speed of the moving front, that control the particle movement. By controlling these factors we can control the morphology of the colloid and its physical properties. Such control is necessary to develop

and optimize these colloids for specific applications.

Acknowledgments

This research was supported through INTAS grant 99-00312 and ALCOM grant DMR 89-20147.

-
- [1] T. C. Lubensky, D. Pettey, N. Currier, and H. Stark, Phys. Rev. E **57**, 610 (1998).
 - [2] H. Stark, Euro. Phys. J. B **10**, 311 (1999).
 - [3] D. Andrienko, G. Germano, and M. P. Allen, Phys. Rev. E **63**, 041701 (2001).
 - [4] D. Andrienko, M. P. Allen, G. Skacej, and S. Zumer, Phys. Rev. E **65**, 041702 (2002).
 - [5] B. I. Lev and P. M. Tomchuk, Phys. Rev. E **59**, 591 (1999).
 - [6] P. Poulin, H. Stark, T. C. Lubensky, and D. A. Weitz, Science **275**, 1770 (1997).
 - [7] P. Poulin and D. A. Weitz, Phys. Rev. E **57**, 626 (1998).
 - [8] J. Loudet, P. Barois, and P. Poulin, Nature **407**, 611 (2000).
 - [9] J. Loudet and P. Poulin, Phys. Rev. Lett. **87**, 165503 (2001).
 - [10] V. J. Anderson, E. M. Terentjev, S. P. Meeker, J. Crain, and W. C. K. Poon, Eur. Phys. J. **4**, 11 (2001).
 - [11] V. J. Anderson and E. M. Terentjev, Eur. Phys. J. **4**, 21 (2001).
 - [12] S. P. Meeker, W. C. K. Poon, J. Crain, and E. M. Terentjev, Phys. Rev. E **61**, R6083 (2000).
 - [13] W. Russel, D. Saville, and W. Schowalter, *Colloidal dispersions* (Cambridge University Press, Cambridge, 1989).
 - [14] M. Tintaru, R. Moldovan, T. Beica, and S. Frunza, Liq. Cryst. **28**, 793 (2001).
 - [15] O. V. Kuksenok, R. W. Ruhwandler, S. V. Shiyanovskii, and E. M. Terentjev, Phys. Rev. E **54**, 5198 (1996).
 - [16] J. L. Billeter and R. A. Pelcovits, Phys. Rev. E **62**, 711 (2000).
 - [17] these particles are widely used as spacers in LCD industry Micropearl SP, made of cross-linked copolymer with divinylbenzene as a major component, $\rho = 1.05 - 1.15 \text{ g cm}^{-3}$.
 - [18] typical values for 5CB (room temperature): $K_{11} = 6.4 \cdot 10^{-7} \text{ dyne}$, $K_{22} = 3 \cdot 10^{-7} \text{ dyne}$, $K_{33} = 10 \cdot 10^{-7} \text{ dyne}$, $W \approx 10^{-2} - 10^{-4} \text{ dyne}$, $\sigma \approx 40 \text{ dyne cm}^{-2}$, $\Delta\sigma \approx 10^{-2} - 10^{-3} \text{ dyne cm}^{-2}$ [14], $\eta = 0.81 \text{ P}$, density of the silica particles, $\rho = 2.5 \text{ g cm}^{-3}$, density of the polymer, $\rho = 1.05 - 1.15 \text{ g cm}^{-3}$, packing fraction of the aggregates, $\phi = 0.3 - 0.8$.